Available online at www.sciencedirect.com

SciVerse ScienceDirect

Journal of the European Ceramic Society 32 (2012) 2679–2690

www.elsevier.com/locate/jeurceramsoc

Calcium phosphate porous pellets as drug delivery systems: Effect of drug carrier composition on drug loading and *in vitro* release

Hiva Baradari *, Chantal Damia, Maggy Dutreih-Colas, Etienne Laborde, Nathalie Pécout, Eric Champion, Dominique Chulia, Marylène Viana

Laboratoire Science des Procédés Céramiques et de Traitements de Surface (SPCTS - UMR 6638 CNRS/Université de Limoges), Centre Européen de la Céramique - 12 Rue Atlantis, 87068 LIMOGES CEDEX, France

Available online 10 February 2012

Abstract

Drug loaded porous calcium phosphate bone substitutes are studied for targeted drug delivery applications. In this study, porous hydroxyapatite and beta-tricalcium phosphate pellets were investigated as anti-inflammatory drug carriers and their ibuprofen adsorption and release properties were compared. While the adsorption equilibrium time of 1 h was obtained for both pellets, hydroxyapatite pellets showed a higher adsorption capacity than beta-tricalcium phosphate. The physico-chemical characterisations of loaded pellets confirmed an ibuprofen reversible physisorption on both hydroxyapatite and beta-tricalcium phosphate pellets. Moreover, higher adsorption capacity of hydroxyapatite was attributed to their physical differences. The *in vitro* ibuprofen release evaluation showed 100% release of ibuprofen from both hydroxyapatite and beta-tricalcium phosphate pellets which was found to be compatible with the obtained interactions between the pellets and ibuprofen.

Keywords: Hydroxyapatite; Beta tricalcium phosphate; Porous pellets; Drug delivery system; Ibuprofen

1. Introduction

Owing to their chemical composition close to the composition of human hard tissues, calcium phosphate (CaP) ceramics are biocompatible and have been used as bone substitutes. Indeed, these bioceramics are suitable for orthopaedic applications because of their ability to form strong bonds with the host bone tissues.[1] In the case of porous CaP, the presence of macroporosity (pore size >80–100 μm) favours the bone formation inside the pores, enhances mechanical interlocking between host tissue and scaffold, while their microporosity (pore size <10 μm) permits the transport of nutrients and metabolic waste by circulation of by biological fluids and together they increase the degradability.[2–4]

After a surgical procedure to restore the bone function in fractures or skeletal deficiencies from trauma, tumors or bone diseases, the appearance of postoperative problems, *i.e.* infection and inflammation, is quite common. But, systemic administration of antibiotics or anti-inflammatories is not effective because of the poor perfusion of diseased bone site. This kind of administration could also cause an increase in drug toxicity to other sites.[5–7] Thus, one of the new challenges in the elaboration of porous CaP ceramics is to use them as drug vehicles for *in situ* drug administration. Therefore, porous CaP implants in combination with drug substances can act as bone substitute and drug carrier during the bone repair procedure, thought decreasing the risks of drug side effects.

For the development of a calcium phosphate based drug delivery system (DDS), it is essential to understand the effect of their chemical and physical parameters on drug/drug carrier interactions and their influence onto the drug release. CaP ceramics cover a wide range of compositions such as Monocalcium phosphate (MCP, $Ca(H_2PO_4)_2{\cdot}H_2O$, Ca/P = 0.5), α-tricalcium phosphate (α-TCP, α-$Ca_3(PO_4)_2$, Ca/P = 1.5), β-tricalcium phosphate (β-TCP, β-$Ca_3(PO_4)_2$, Ca/P = 1.5), hydroxyapatite (HA, $Ca_{10}(PO_4)_6.(OH)_2$, Ca/P = 1.667) and biphasic calcium phosphates (BCP) consisting of a mixture of HA and β-TCP. These materials have very different dissolution properties due to their different chemistry and crystalline structure.[8] As a consequence, they may provide different drug loading and release properties. Depending on the carrier chemical composition, the adsorbed amount of a drug can be modified.[9] Besides, the drug molecule can be adsorbed reversibly or irreversibly onto carrier and as a result different released amount of a drug can be

* Corresponding author. Tel.: +33 5 87 50 23 64.
E-mail address: hiva.baradari@etu.unilim.fr (H. Baradari).

0955-2219/$ – see front matter © 2012 Elsevier Ltd. All rights reserved.
doi:10.1016/j.jeurceramsoc.2012.01.018

obtained.[10] Physical properties of carrier like its specific surface area or pore network can also directly affect the adsorbed amount of drug and its release rate.[11]

Ibuprofen is one of the most widely used non-steroidal anti-inflammatory model drug in DDS studies because of its short biological half-life (2 h) and good pharmacological activity. As above mentioned, adding an anti-inflammatory drug in porous CaP ceramics can attenuate the local inflammatory response due to the implantation process. Such DDS can also be used for the local treatment of articular inflammatory pathologies such as arthritis. The combination of ibuprofen and its interaction with inorganic porous carriers for local drug delivery have been reported mostly in the case of mesoporous carriers.[12–14] But, only few studies have reported ibuprofen loading and release properties of CaP scaffolds.[15,16]

The present work focuses on the study of the effect of CaP porous pellets chemical composition on ibuprofen adsorption and release behaviour. For this aim, two CaP ceramics, HA and β-TCP, were chosen. After elaboration of HA and β-TCP porous pellets by wet high shear granulation method,[17,18] the obtained pellets were loaded by impregnation in ethanol solutions of ibuprofen in order to compare HA and β-TCP loading kinetics and ibuprofen adsorption capacities.[19] The interactions between ibuprofen and CaP pellets were studied by X-ray diffraction, FT-IR spectroscopy and Raman diffusion. The ibuprofen release profile was then obtained in phosphate buffer solution at 37 °C and the dissolution mechanisms of ibuprofen loaded on HA and β-TCP pellets were compared.

2. Materials and methods

2.1. Porous pellets fabrication

Tricalcium phosphate powder ($Ca_3(PO_4)_2$ – Cooper, France) was purchased in order to prepare beta tricalcium phosphate (β-TCP-$Ca_3(PO_4)_2$) pellets. Based on primary characterisations, this commercial powder has a specific surface area of 30 $m^2\ g^{-1}$ and a particle size of 9 μm ($d_{0.5}$).[20]

Hydroxyapatite (HA – $Ca_{10}(PO_4)_6(OH)_2$) was synthesized in the laboratory by the hydrothermal route. After fixing the molar ratio of precursors at 1.677, an aqueous solution of diammonium phosphate ($(NH_4)_2HPO_4$ – Aldrich, France) was added to a calcium nitrate tetra-hydrate solution ($Ca(NO_3)_2{\cdot}4H_2O$ – Aldrich, France) at a rate of 40 mL min^{-1}. The details of synthesis process are explained elsewhere.[21] The obtained powder was then calcined at 650 °C during 30 min in order to obtain a powder with similar specific surface area as the tricalcium phosphate commercial powder. Calcined HA powder had a surface specific area of 34 $m^2\ g^{-1}$ and a particle size of 10 μm ($d_{0.5}$).

Porous calcium phosphate (CaP) pellets were fabricated by wet high shear granulation method followed by spheronisation in a Mi-Pro high shear granulator (Pro-C-epT, Zelzate, Belgium).[17] Pregelatinised starch (Sepistab ST 200, Seppic, France) was used as binder/pore former. The volume of granulation liquid, *i.e.* distilled water, was adjusted to liquid/powder (L/P) ratios of 93/200 and 115/200 mL g^{-1} for TCP and HA respectively. The obtained CaP granules were dried in a fluidised bed dryer (Glatt, Haltingen Binzen/Baden, Germany) during 20 min at 60 °C and sieved in order to retain the 710–1000 μm fraction.

The pellets were first heat treated at 270 °C during 2 h to eliminate the pore former,[20] and then calcined at 900 °C/15 min for TCP and 950 °C/15 min for HA (furnace Vecstar Ltd., United Kingdom) to obtain pellets with similar specific surface areas and improved mechanical properties.

2.2. Drug loading

Ibuprofen 50 ($C_{13}H_{18}O_2$ – BASF, Germany) was used as the therapeutic agent. The adsorption experiments were performed in triplicate by soaking 350 mg of porous pellets in ibuprofen ethanolic solutions (technical ethanol – 96 wt.%) under ambient atmosphere and at room temperature, without agitation. After a given contact time, loaded granules were separated from their supernatant and dried overnight at room atmosphere and temperature. Ibuprofen loading was performed according to two different regimes:

(1) soaking the pellets in 4 mL of a 100 mg mL^{-1} ibuprofen solution from 10 min to 24 h to obtain the adsorption kinetics and
(2) soaking the pellets for 1 h in 4 mL of ibuprofen solutions with concentrations from 50 mg mL^{-1} to 300 mg mL^{-1} for studying the adsorption at room temperature.

The adsorbed amount of ibuprofen was quantified *via* direct measurement method. Based on the high solubility limit of ibuprofen in ethanol, *i.e.* 428 mg mL^{-1} at 20 °C,[22] the loaded pellets were immersed in 40 mL of ethanol during 4 h. Eluted ibuprofen concentration was measured by UV absorption spectrophotometry (Lambda 20 spectrophotometer, Elmer Perkin, USA) at λ = 264 nm. The adsorbed amount (Q) of ibuprofen was deduced from Eq. (1):

$$Q\ (\text{mmol m}^{-2}) = \frac{\text{Adsorbed ibuprofen quantity (mmol)}}{\text{Sample mass (g)} \times \text{Specific surface area (m}^2\,\text{g}^{-1})} \quad (1)$$

The drug content (DC%) was calculated according to Eq. (2):

$$\text{DC\%} = \left[\frac{\text{Adsorbed ibuprofen mass (mg)}}{\text{Loaded sample mass (mg)}}\right] \times 100 \quad (2)$$

2.3. In vitro ibuprofen dissolution kinetics

Dissolution tests[23] were performed on pellets loaded with a solution of ibuprofen at 200 mg mL^{-1} during 1 h. Un-loaded pellets were used as reference. Trials were carried out, using a phosphate buffer solution (pH = 7.5) at 37 °C as dissolution medium. The dissolution tests were performed using the flow-through cell apparatus, described in European Pharmacopea,[24] equipped with tablet cells of 12 mm. A ruby bead of 5 mm diameter and glass beads of 1 mm diameter were placed in the apex

of the flow-through cell in order to ensure laminar flow of the 100 mL of dissolution medium, in a close circuit (*i.e.* constant volume of 100 mL of the dissolution medium), entering into the cell with a flow rate of 2 mL min^{-1}. 275 mg of accurately weighted loaded granules were placed on the glass bead bed. The automated system CE 7smart (Sotax, Basel, Switzerland) was linked to a piston pump CP7-35 (Sotax, Basel, Switzerland) and a UV-visible spectrophotometer (Lambda 20, Perkin Elmer, USA) for a direct online analysis of the filtered samples. Ibuprofen released amount was determined at regular intervals at $\lambda = 264$ nm.

Dissolution profile, *i.e.* cumulative percentage of released ibuprofen *versus* time (min), was then plotted. In order to determine the release mechanism, results were fitted to two mathematical models, characterising diffusion and erosion prevalence, respectively, the Higuchi equation (Eq. (3))[25]:

$$q(\%) = at^{1/2} + b \tag{3}$$

where a is the release rate (%/$h^{1/2}$) and b a constant; and the Hixson–Crowell model (Eq. (4))[26]:

$$\sqrt[3]{100} - \sqrt[3]{100 - q} = c \times t \tag{4}$$

where c is the release rate and q is the drug released %.

2.4. Physico-chemical characterisations

X-ray powder diffraction patterns were collected by means of Cu Kα radiation ($\lambda = 1.5406$ Å) on a $\theta/2\theta$ diffractometer (D8, Bruker) with a step size of 0.02° and a count time of 2 s. Phase identification was processed on EVA software (Bruker AXS) by comparing the diffraction patterns with the International Center for Diffraction Data (ICDD) Powder Diffraction Files (PDF): 00-09-0432 for hydroxyapatite – HA, 00-09-0169 for beta-tricalcium phosphate – β-TCP and 00-034-1728 for ibuprofen. Fourier Transformed Infra-Red spectroscopy (FTIR) (Spectrum One, Perkin-Elmer) was performed on samples prepared by mixing granules (1 wt.%) with KBr powder. The spectra were collected in the range of 4000–400 cm^{-1} at the ambient temperature, with a resolution of 2 cm^{-1}. Raman spectra were obtained over the 250–3700 cm^{-1} range, using a Raman spectrometer (Jobin Yvon – Argon-ion laser at 514,532 nm – Stabilite 2017 Spectra physics).

Morphological investigation was performed using a field emission gun scanning electron microscope (FEG-SEM, Jeol JSM-7400 F) without sputter-coating of samples. Specific surface area (SSA, $m^2\ g^{-1}$) was measured by nitrogen adsorption using a Gemini 2360 Analyser (Micromeritics Instruments Inc.) and calculated according to the Brunauer–Emmet–Teller equation.[27] Samples were previously degassed for 3 days at 30 °C at a pressure lower than 50 mTorr (VacPrep 061, Micromeritics Instruments Inc.).[28] Measurements were repeated until stabilisation of the SSA value. Porosity measurements were carried out using a mercury intrusion porosimeter (Autopore IV 9500; Micromeritics Instruments Inc.) equipped with a 5 cm^3 powder penetrometer. Cumulative and incremental mercury intrusion volumes were recorded. The intrusion volume (V_{intra}, mL g^{-1}) corresponding to pellet open porosity was deduced and associated with the corresponding pore size diameters. Pellets total porosity (%) was calculated according to Eq. (5):

$$\text{Pellets total porosity } (\%) = \frac{V_{intra}}{V_{solid} + V_{intra}} \times 100 \tag{5}$$

where V_{solid} is the solid volume, determined from the pycnometric density.

The zeta potential (ζ – mV) of the CaP pellets as a function of ibuprofen concentration in ethanol was measured with a Zetasizer Nano ZS90 (Malvern Instruments, UK). For evaluation of pellets zeta potential, suspensions were prepared by dispersing 50 mg of grinded CaP pellets in technical ethanol and ethanolic solutions of ibuprofen (50,100 and 200 mg mL^{-1}) by magnetic agitation, without addition of dispersants. Suspensions were kept still more than 1 h to stabilise them and then, the supernatant was taken off to perform the zeta potential measurements on it.

In order to investigate the possible dissolution of the CaP pellets during the drug loading procedure and the *in vitro* dissolution trials, Ca^{2+} content of the impregnation solutions and the dissolution medium (phosphate buffer) was quantified *via* cresolphthalein complexone (CPC) method.[29] The purple Ca-CPC complex was detected by UV absorption spectrophotometry (Lambda 20, Perkin Elmer, USA) at 575 nm and the Ca-CPC complex concentration was attributed to Ca^{2+} concentration of the impregnation solutions and phosphate buffer.

3. Results

3.1. CaP pellets characteristics

XRD patterns of β-TCP and HA pellets after the heat treatment at 900 °C and 950 °C respectively, show that pellets are mainly composed of well-crystallised β-TCP and HA (Fig. 1).

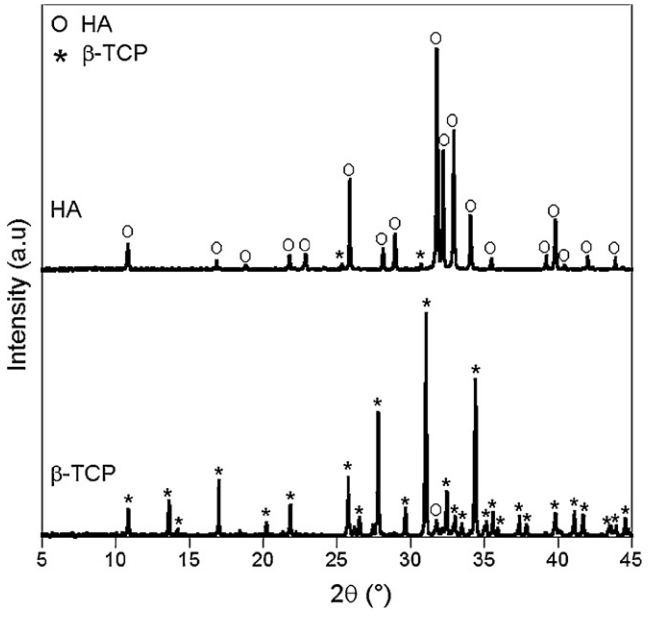

Fig. 1. XRD patterns of HA and β-TCP pellets calcined at 950 °C and 900 °C, respectively.

A slight trace of HA is observed in β-TCP pellets and traces of β-TCP are present in HA pellets. Quantification of HA and β-TCP phases[30] indicates that the global Ca/P molar ratio of β-TCP pellets is equal to 1.512 and the one of HA pellets is equal to 1.662.

The presence of HA in β-TCP pellets was stemmed from the initial commercial powder. It was primarily composed of 80 wt.% dicalcium phosphate anhydrate (DCPA, $CaHPO_4$) and 20 wt.% hydroxyapatite[20]; the heat treatment at 900 °C resulted in their transformation into stable β-TCP phase with residual HA. The Ca/P molar ratio of HA pellets (1.662) indicates that the powder obtained from hydrothermal synthesis was lightly calcium-deficient hydroxyapatite (Ca-dHA). During HA synthesis by hydrothermal route, it is possible to process a biphasic product containing HA and β-TCP by heating Ca-dHAP that has the same crystal structure as stoichiometric HA with a Ca/P ratio ranging from 1.5 to 1.667 ($Ca_{10-x}(PO_4)_{6-x}(HPO_4)_x(OH)_{2-x}$ with $0 < x < 1$).[31]

Fig. 2a shows the FT-IR spectra of the calcined pellets. The phosphate (PO_4) vibration modes (ν_1, ν_2, ν_3 and ν_4) are visible on CaP calcined pellets spectrum. The ν_2 of P–O–P bending appears only on HA spectra at 474 cm^{-1}. The ν_4 of P–O bond are present as bands at 571 cm^{-1} and 601 cm^{-1} on HA and at 551 cm^{-1} and 608 cm^{-1} on β-TCP spectra. The ν_1 symmetric stretching of P–O bond is visible at 962 cm^{-1} on HA spectrum and this bond appears at 947 and 969 cm^{-1} on β-TCP spectrum. The bands at 1043 cm^{-1} and 1089 cm^{-1} on HA and at 1039 cm^{-1} and 1121 cm^{-1} on β-TCP spectra are assigned to ν_3 of P–O bond. Additionally, the absorption bands assigned to OH group of hydroxyapatite are present at 3575 cm^{-1} and 630 cm^{-1} on HA spectrum.[31]

Raman spectra of CaP porous pellets are illustrated in Fig. 2b. The bands originating from the ν_2 of HA are spanned over the frequency range of 400–503 cm^{-1} and those of β-TCP are present over a frequency range of 370–500 cm^{-1}. The ν_4 bending modes of the PO_4 group (O–P–O bond) of HA and β-TCP are present at the frequency ranges of 574–657 cm^{-1} and 530–645 cm^{-1} on their spectra, respectively. The peak arising from stretching mode (ν_1) of the PO_4 group (P–O bond) is detected at 962 cm^{-1} on HA and at 967 and 948 cm^{-1} on β-TCP spectra. The ν_3 mode of PO_4^{3-} of HA is present over 1036–1116 cm^{-1} and over 1030–1100 cm^{-1} on β-TCP spectrum. The bond-stretching mode associated with the OH group of HA pellets is also detected as a sharp peak at 3571 cm^{-1}.[32]

Table 1
Physical properties of HA and β-TCP pellets calcined at 950 °C and 900 °C, respectively.

Sample	Porosity (%)	SSA ($m^2\ g^{-1}$)
HA	67	6.3
β-TCP	57	5.4

The surface morphology of the pellets is presented in Fig. 3. Pores larger than 1 μm in diameter, with random shapes, are present on the surface of the CaP pellets. The random pores shape of the surface of the pellets is due to the elimination of agglomerated pore former powder. The presence of pores smaller than 1 μm, is attributed to the rearrangement of HA and β-TCP particles during the sintering at 950 and 900 °C. After the coalescence of the CaP particles and the formation of necks between them during the heat treatment, the small pores are formed.[33]

Physical properties of the obtained pellets, total porosity and their specific surface area (SSA) are presented in Table 1. The wet high shear granulation method followed by heat treatment resulted in the formation of porous pellets with close specific surface areas. As it can be seen from pore size distribution diagram (Fig. 9), a bimodal pore distribution is obtained for both HA and β-TCP pellets, which is compatible with morphological observations. This bimodal pore size distribution is classified into first category of pores defined from 80 to 300 nm for β-TCP and 70–400 nm for HA, and second category considered from 300 to 2000 nm and 400–6000 nm for β-TCP and HA, respectively. Although the same amount of pore former was used for both composition granulation, the total porosity of HA pellets is higher than β-TCP pellets one.

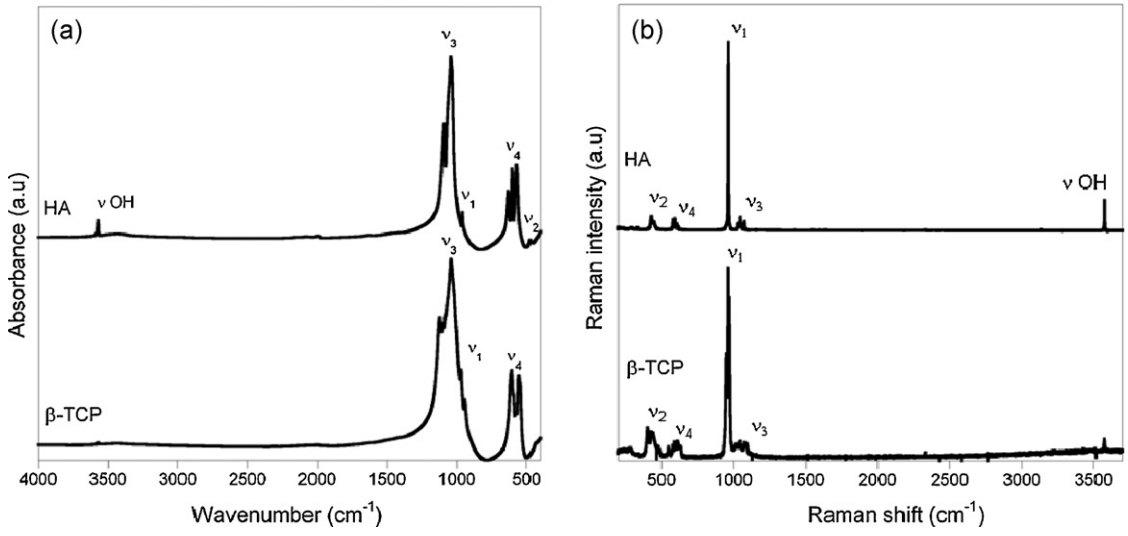

Fig. 2. (a) FTIR and (b) Raman spectra of HA and β-TCP pellets calcined at 950 °C and 900 °C, respectively.

The pellets in size fraction of 710–1000 μm creates an intergranular macroporosity of about 180 μm, suitable for bone ingrowth[18] and intragranular bimodal microporosity which allows these pellets to be loaded with a drug molecule.

3.2. Drug adsorption behaviour

The drug adsorption was performed by varying two parameters: ibuprofen adsorption time to provide ibuprofen adsorption kinetics and the initial concentration of ibuprofen solutions (C_0) to obtain informations on the adsorption mechanisms.

Fig. 4a shows the adsorption kinetic curves of ibuprofen ($C_0 = 100\,mg\,mL^{-1}$). The drug adsorption trend is similar for both pellets composition and the threshold of adsorption is obtained from 1 h for HA and β-TCP pellets, corresponding to DC% of $6.46 \pm 0.47\%$ and $5.18\% \pm 0.14\%$, respectively. Therefore, one hour is considered as the equilibrium time (t_{eq}) of adsorption for both compositions. Therefore, 1 h was uses as the contact time for the rest of the adsorption experiments.

The adsorption curves are presented in Fig. 4b. In the considered ibuprofen concentration range the obtained adsorption curves show a linear correlation between DC% and the initial concentration of the drug solution without reaching a plateau. Adsorption curves fit to Freundlich equation, defined by $Q = aC_e^m$ where Q corresponds to the adsorbed drug amount ($mmol\,m^{-2}$), C_e is the equilibrium concentration of ibuprofen in the adsorption solutions ($mmol\,mL^{-1}$), a and m are Freundlich equation constants reflecting the adsorption capacity and adsorption affinity, respectively.[34] Freundlich equation constants were determined by linearising the equation ($\ln Q = \ln a + m \ln C_e$).

Table 2
Freundlich adsorption constants of HA and β-TCP calcined pellets for adsorbed ibuprofen.

Sample	Freundlich constants		
	a	m	R^2
HA	0.12	1.20	0.9889
β-TCP	0.10	0.91	0.9959

The numerical values for m and a are reported in Table 2. As it can be seen, both the adsorption affinity (m) and the adsorption capacity (a) of HA pellets are found to be higher than the adsorption constants of β-TCP pellets. The ibuprofen desorption of both HA and β-TCP pellets was also studied (data not shown). The superimposition of the obtained desorption curves with the adsorption ones, following the same linear trend indicates that the ibuprofen adsorption on both HA and β-TCP pellets is reversible.

Fig. 5 presents the zeta potential (ζ) charges of the pellets surface as a function of the concentration of ibuprofen solution, C_0. The pellets are found to be positively charged in ethanol with similar charges of $\zeta_{HA} = 10.37 \pm 0.43\,mV$ and $\zeta_{\beta\text{-TCP}} = 11.46 \pm 0.56\,mV$. As it can be seen, the pellets charge decreases by increasing the concentration of ibuprofen. Moreover, the rate of electrical charge decrease is found to be the same for both HA and β-TCP pellets.

In order to evaluate the dissolution rate of CaP pellets during the ibuprofen loading and to understand the effect of drug loading method on pellets possible evolution, the calcium content of ibuprofen solution ($200\,mg\,mL^{-1}$) after 1 h of contact

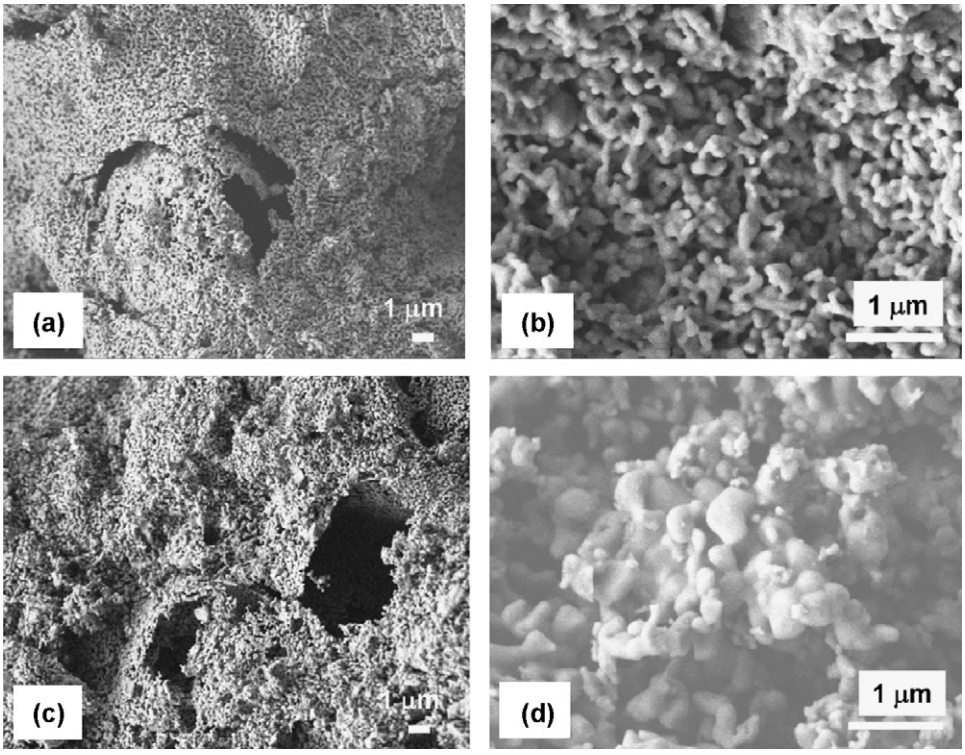

Fig. 3. FEG-SEM images of (a), (b) HA and (c), (d) β-TCP pellets after calcination at 950 °C and 900 °C, respectively.

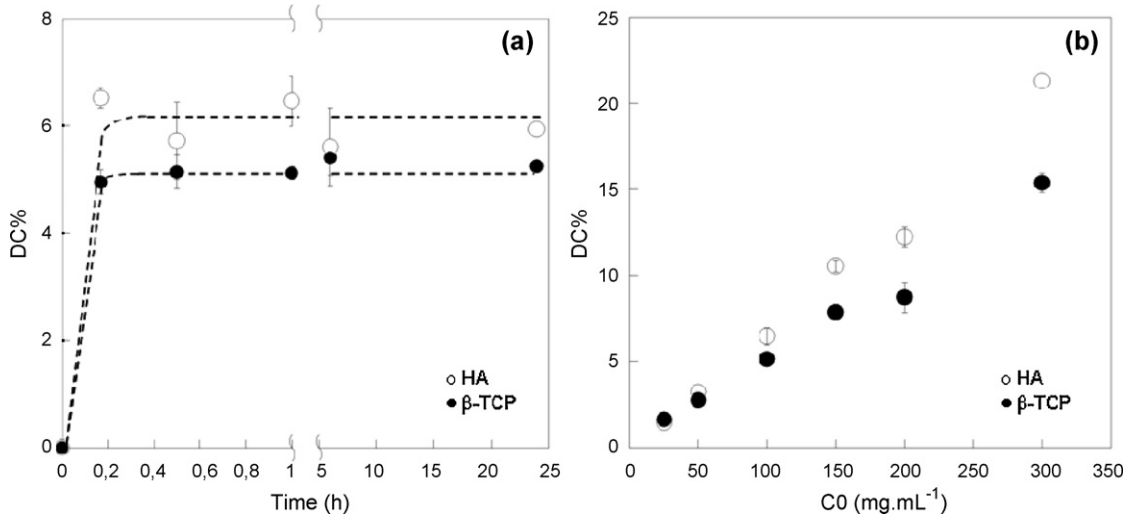

Fig. 4. (a) Adsorption kinetics and (b) adsorption curves of ibuprofen on HA and β-TCP calcined pellets.

with the pellets was measured. The calcium concentration of the adsorption solutions at t_{eq} of HA pellets is equal to that of β-TCP, corresponding to 5×10^{-4} mmol mL^{-1}, compatible with the solubility value of HA and β-TCP in water.[31] Hence, only slight dissolution of the pellets occurred during the impregnation.

3.3. Ibuprofen loaded CaP pellets characteristics

Pellets loaded by 200 mg mL^{-1} ibuprofen solution were submitted to further physico-chemical characterisations in order to locate ibuprofen on the pellets and to determine the type of interactions between the drug and the carrier.

The XRD patterns of the loaded pellets and ibuprofen are illustrated in Fig. 6. The initial ibuprofen powder presents a crystalline structure. The most intense diffraction peaks of ibuprofen are present on diffraction pattern of both HA and β-TCP pellets, indicating that ibuprofen was adsorbed onto the pellets under its crystalline form. It can be observed that HA and β-TCP pellets kept also their initial crystalline structure (see Fig. 1), that is to say the contact of pellets with the impregnation medium (*i.e.* ibuprofen solution of 200 mg mL^{-1}) did not modify their bulk crystalline structure.

The FTIR spectra of ibuprofen and loaded CaP pellets are displayed in Fig. 7a. The characteristic PO_4^{3-} bands of β-TCP and HA are found on the loaded pellets spectra (see Fig. 2a). The C–H_x stretching bands (ν C–H_x) around 3000–2850 cm^{-1} and the band assigned to the C=O elongation mode (ν COOH) of –COOH group at 1720 cm^{-1} confirm the adsorption of ibuprofen onto CaP pellets.[19]

The characteristic bands of ibuprofen are more visible on the Raman spectrum of the loaded pellets (Fig. 7b). Similar to

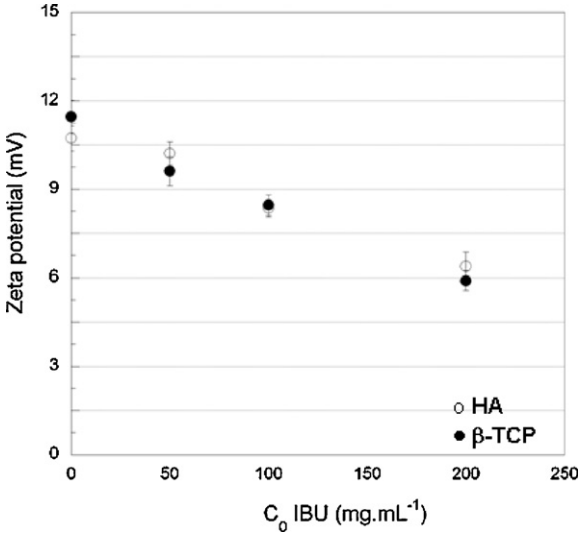

Fig. 5. Zeta potential as a function of ibuprofen ethanolic solution concentration for HA and β-TCP calcined pellets.

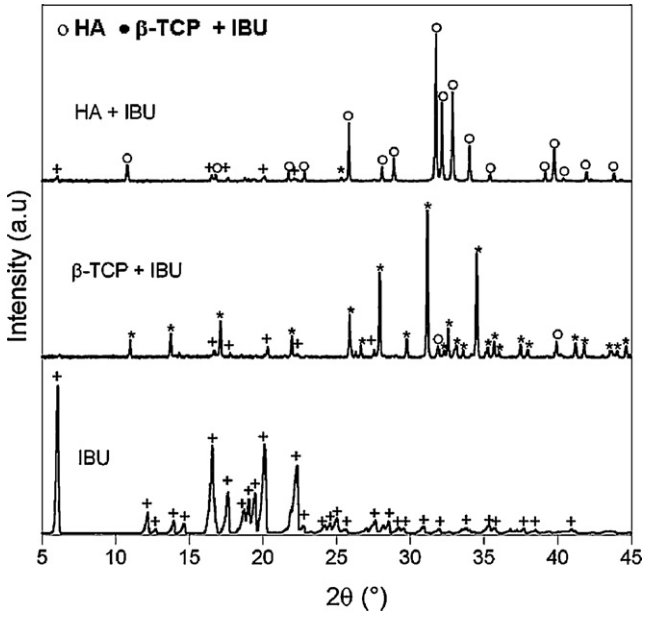

Fig. 6. XRD patterns of (IBU) ibuprofen and (HA + IBU) HA and (β-TCP + IBU) β-TCP pellets loaded with ibuprofen.

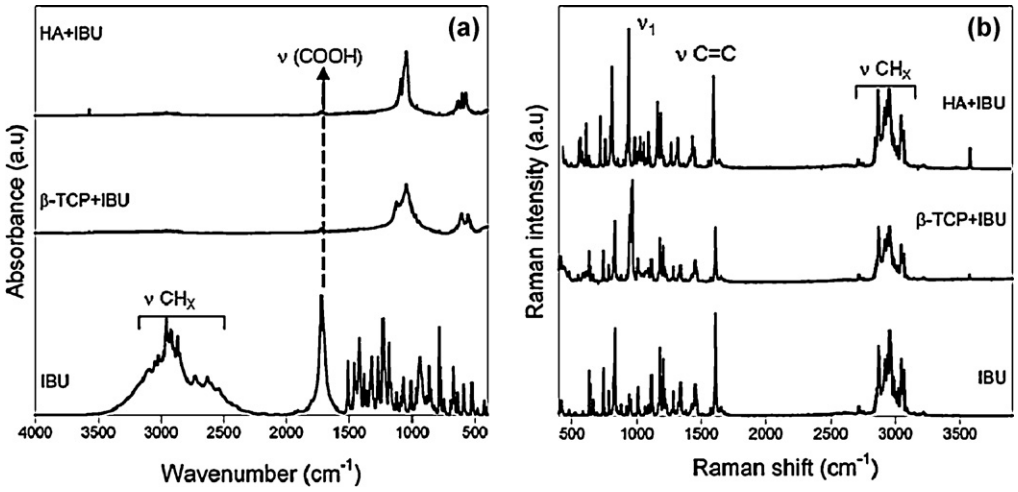

Fig. 7. (a) FTIR and (b) Raman spectra of ibuprofen (IBU) and (HA + IBU) HA and (β-TCP + IBU) β-TCP pellets loaded with ibuprofen.

pure ibuprofen Raman spectrum, the stretching bands of C–H_x (ν C–H_x) between 3100 and 2700 cm^{-1}, consisting of symmetric and antisymmetric stretching vibration of =C–H and –C–H, are present on loaded pellet spectra. The ν C=C at 1608 cm^{-1} is also similar to that on the Raman spectrum of pure Ibuprofen. Amongst Raman intensities from 1470 to 637 cm^{-1}, O–H bending modes of COOH function (*i.e.* δ(C(O)O–H)), at 1432, 1227, 1124, 662 and 637 cm^{-1} are present on loaded pellet spectra, indicating that ibuprofen is adsorbed on HA and β-TCP pellets under its acidic form.

As shown in Fig. 8, ibuprofen is adsorbed as fine crystalline filaments on both HA and β-TCP surface and it did not keep its initial morphology of rod like crystals.

The physical properties of the pellets before and after loading are compared in Table 3. The decrease of specific surface area of the pellets is similar for both compositions. The drug adsorption results in 13% and 11% decrease of specific surface area of HA and β-TCP pellets, respectively. The decrease of the porosity (total porosity, 1st and 2nd category pore volume), in the case of HA pellets, is more noticeable than that of β-TCP pellets (Fig. 9). Moreover, the pores volume of the 1st category decreases more than the large ones for both types of pellets.

3.4. In vitro ibuprofen dissolution kinetics

Dissolution profiles, *i.e.* cumulative percentage of ibuprofen released (wt.%) *versus* time, are plotted in Fig. 10. The ibuprofen-CaP porous pellets system exhibits a fast release of ibuprofen within the mentioned experimental conditions. The lag time of about 3 min is due to the time required to obtain a homogenous drug substance distribution in the release medium. The ibuprofen release profile consists of two phases: a fast release of about 70% of adsorbed ibuprofen for β-TCP pellets and 75% for HA pellets in the first 15 min, followed by a slow release of the remaining adsorbed ibuprofen. The necessary time to release 90% of adsorbed ibuprofen is around 10 min in the case of HA pellets and 15 min in the case of β-TCP pellets. The plateau of release takes about 70 min for both compositions. These results confirm the ability of calcium phosphate porous pellets drug delivery system in complete ibuprofen release.

The dissolution data were adjusted to Higuchi and Hixson–Crowell equations in order to determine the release mechanism. The drug dissolution kinetics data of the first and second phase of release were linearised separately. The correlation coefficients (R^2) are given in Table 4. The comparison between the correlation coefficients of HA and β-TCP pellets indicates that data of both release phases are better fitted to Hixson–Crowell. Thus, it can be suggested that the release of ibuprofen is controlled by drug erosion from surfaces of both pellet compositions.

The porous pellets possible chemical changes after being in contact with phosphate buffer at 37 °C were controlled. For this aim, loaded HA and β-TCP pellets after ibuprofen release in phosphate buffer and non-loaded HA and β-TCP pellets used

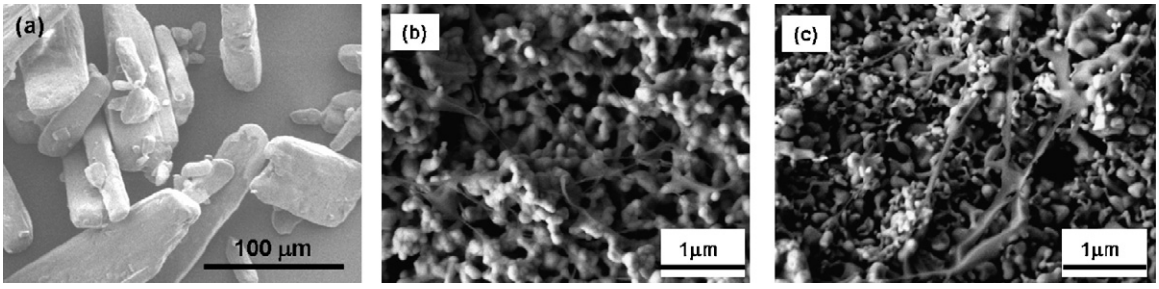

Fig. 8. FEG-SEM images of (a) initial ibuprofen, (b) HA and (c) β-TCP pellets loaded with ibuprofen.

Table 3
Physical properties of HA and β-TCP pellets before and after ibuprofen adsorption.

Sample	SSA ($m^2\,g^{-1}$)	Total porosity (%)	Total pore volume ($mL\,g^{-1}$)	1st category volume ($mL\,g^{-1}$)	2nd category volume ($mL\,g^{-1}$)
HA	6.3	65	0.61	0.38	0.23
HA + IBU	5.5	44	0.25	0.13	0.10
β-TCP	5.4	57	0.45	0.35	0.10
β-TCP + IBU	4.8	50	0.33	0.25	0.08

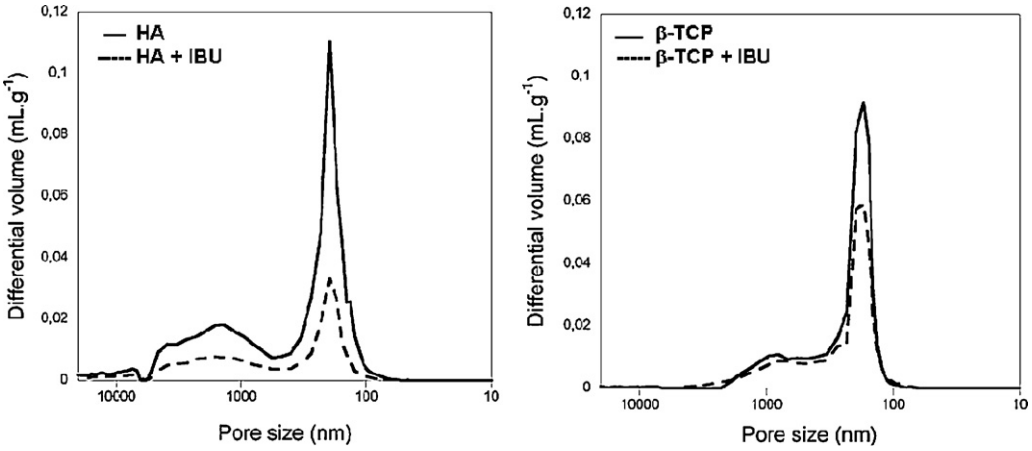

Fig. 9. Pore size distribution of HA and β-TCP calcined pellets before (plain line) and after (dashed line) drug loading.

Table 4
Modelled drug dissolution characteristics.

Sample	HA		β-TCP	
Drug release phase	1	2	1	2
Time (h)	0–0.25	0.25–0.40	0–0.25	0.25–0.46
Higuchi R^2 coefficient	0.9954	0.9644	0.9904	0.9955
Hixson–Crowell R^2 coefficient	0.9974	0.9802	0.9947	0.9994

as reference (*i.e.* in contact with the medium under the same conditions) were characterized by FT-IR and XRD. The calcium content of phosphate buffer at the end of release test was also measured.

The XRD patterns (Fig. 11a) of the pellets show no trace of ibuprofen after ibuprofen release trials. It can also be seen that HA and β-TCP kept their crystalline structure (cf. part 3-1) and no new crystalline phase was formed during the period of contact (4 h) with the medium. The FTIR spectra of the same pellets (Fig. 11b) indicate the same results; neither reference pellets nor pellets after ibuprofen desorption, were modified chemically during the process. Moreover, the measurement of the calcium concentration of phosphate buffer solutions at the end of the dissolution test did not show the presence of Ca^{2+} ions in the solutions, indicating that no pellets dissolution occurred in the release medium.

4. Discussion

The feasibility of β-TCP porous pellets production by wet high shear granulation method, using them as bone fillers and

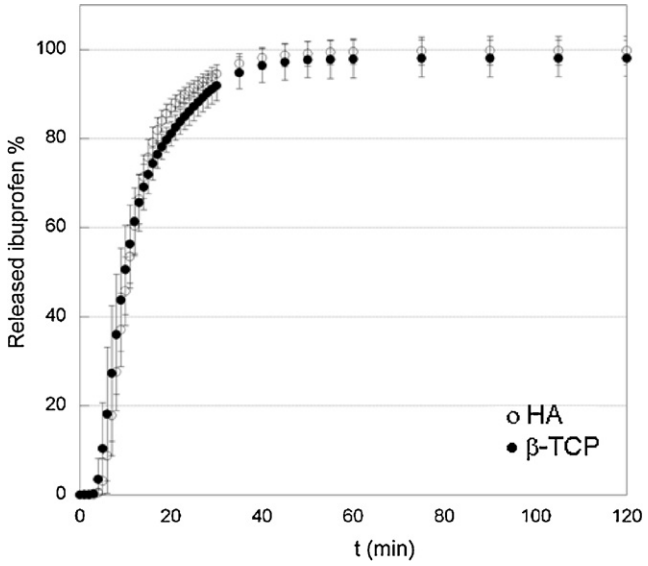

Fig. 10. Ibuprofen dissolution kinetics for (◯) HA and (●) β-TCP pellets.

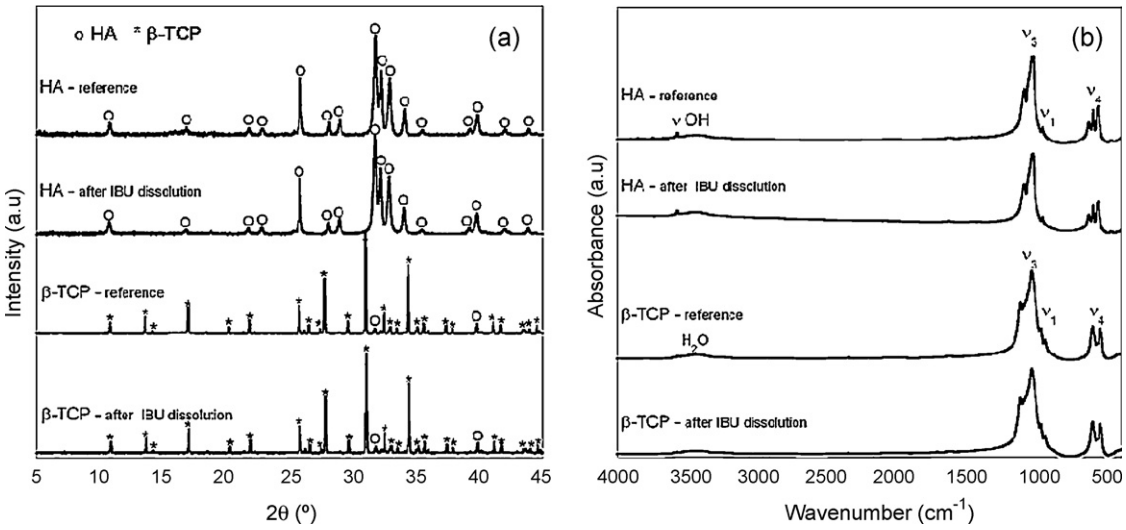

Fig. 11. (a) XRD patterns and (b) FTIR spectra of HA and β-TCP pellets after ibuprofen (IBU) dissolution.

ibuprofen carriers in orthopaedic field has been shown in previous works.[17,18–35] The present study focuses on the effect of the porous pellets chemical composition on the ibuprofen adsorption mechanism and *in vitro* release kinetics. For this aim, HA and β-TCP were chosen as two compositions of calcium phosphate materials family having different solubilities.

The granulation and heat treatment parameters were adjusted in a way to obtain pellets with similar physical properties such as specific surface area and total porosity, in order to decrease the influence of physical parameters on the drug adsorption and release. Although the same amount of pore former was used, the obtained total porosity of HA pellets was 10% higher than that of β-TCP, with higher volume of two categories of pores. This difference in porosity stems from the granulation, as the agglomeration mechanisms are very complex and particularly depend on the physico-chemical characteristics of the particles[36–38] and/or from the heat treatment.[33] Therefore, the resulting pore network, morphology, distribution and size could differ from one composition to another. Thus, besides considering the chemical composition, the total porosity of the pellets is also taken into account for further discussions on the observed differences between the drug adsorption capacity of HA and β-TCP porous pellets.

The adsorption kinetics study is important to understand the rate at which adsorption takes place. Generally speaking, the adsorption plateau of an adsorbate from a liquid phase to adsorbent surface can be obtained after establishing equilibrium between the solution and the solid phase.[39] Based on a previous work[19] and a work by Stahli et al.,[40] in the case of porous substrates in contact with a liquid phase, this equilibrium is established after saturating the open pores through capillary rise of the liquid phase. Therefore, the adsorption equilibrium time of ibuprofen adsorption onto HA and β-TCP pellets can be related to the required time to fill the open pores by the drug solution and the rate of capillary rise through open pores of the pellets. The results of measuring the effect of contact time on ibuprofen adsorption on CaP porous pellets revealed that the drug adsorption is fast and the equilibrium is achieved after 1 h of contact time, regardless of pellets chemical composition. It can be deduced that the pore filling is the result of the drug solution penetration inside the porous network and the drug deposition, after solvent evaporation. The more the drug solution is concentrated, the more the amount of drug in the porous network is significant. Although the same saturation times (t_{eq}) were obtained for both pellet compositions, the rate of pore filling in HA pellets was found to be higher than the one of β-TCP pellets (see part 3-3). That is to say, a higher volume of ibuprofen solution has penetrated into HA pellets. This result can be due to either a higher affinity of ibuprofen solution for HA pellets or a different pore network structure of these pellets from β-TCP ones. In order to better understand this point, the adsorption mechanisms and physico-chemical characteristics of the loaded pellets are discussed below.

The obtained adsorption data were fitted to the Freundlich adsorption model which is one of the well-known adsorption equilibrium mathematic models. This adsorption model reflects an adsorption following a heterolayer formation of adsorbate; this result is compatible with the surface morphology of the loaded pellets (Fig. 8). Analysing the obtained experimental data by this equation shows that the adsorption capacity of HA pellets (0.12 mL m^{-2}) is slightly higher than the one of β-TCP (0.10 mL m^{-2}), which is compatible with the higher DC% obtained at C_0 of 200 mg mL^{-1} for HA pellets (12.23%) than for β-TCP pellets (8.72%).

The difference in the adsorption capacity of an adsorbent, here drug carrier, can originate from several parameters like carriers chemical composition, surface charges,[9] pore network[41] and pores tortuosity,[16] specific surface area.[42] Physico-chemical characterisations of ibuprofen loaded pellets were performed in order to understand the reason behind the higher adsorption capacity of HA pellets than β-TCP pellets. Ibuprofen is a polar molecule with acidic properties, able to be present under a deprotonated form in a water/alcoholic medium and adsorbed on a substrate surface through a chemical reaction or ion exchange.

The adsorption of ibuprofen in its acidic form has been evidenced on Raman spectra of the loaded pellets by the presence of OH bending modes of COOH groups. In the case of the formation of hydrogen bonds between available −OH group of HA and COOH group of ibuprofen[15] a broad band centred at about 3430 cm^{-1} on FT-IR spectra of ibuprofen loaded HA should appear. In the present work, the FTIR and Raman spectra of the loaded HA and β-TCP pellets did not reveal any chemical modification of neither ibuprofen nor HA and β-TCP pellets, indicating that ibuprofen is adsorbed by physisorption on both HA and β-TCP pellets. The decrease of the zeta potential of pellets by increasing the amount of adsorbed ibuprofen indicates that the driving force of ibuprofen physisorption on calcium phosphate pellets is the electrostatic attractions between ibuprofen polar molecule and the pellets positively charged surface. Besides, the erosion of a drug carrier in drug loading medium makes the drug uptake difficult and hence it can change the drug adsorbed amount.[9] Here the measurement of the Ca^{2+} concentration in the impregnation solution showed that HA and β-TCP pellets, based on their solubility values, lightly dissolved during the impregnation procedure. But, as ibuprofen physisorbed onto the pellets, this slight pellets dissolution cannot disturb the drug adsorption. These results reveal that ibuprofen/HA and ibuprofen/β-TCP interactions follow the same mechanism and the difference in their adsorption capacities comes from physical parameters.

The most influencing physical parameters which can affect the adsorption capacity of drug carriers are their specific surface area and their porosity. In order to understand the effect of carrier's surface area on drug uptake, it is common to normalise the adsorption data with respect to carriers specific surface area.[10] After normalising the adsorbed amount (Q) of ibuprofen with the specific surface area of HA and β-TCP pellets, difference in adsorption capacities are still observed. Therefore, the higher adsorption capacity of HA pellets could be attributed to their higher total porosity than that of β-TCP pellets. To withdraw the influence of the pore network on ibuprofen adsorption, HA and β-TCP pellets were grinded and sieved in order to obtain powders which were then loaded by a solution of ibuprofen at concentration of 200 mg mL^{-1} and their drug contents (DC%) were compared: the same DC% of 25% was obtained for both compositions. To sum up, based on the fact that ibuprofen has the physical interaction with HA and β-TCP pellets (physisorption), and both compositions have the same electrical charges in adsorption medium, the reason behind the higher adsorption capacity of HA pellets is supposed to be their higher total porosity. This higher total porosity results in the penetration of a higher volume of drug solution inside open pores and hence, after solvent evaporation, a higher amount of adsorbed drug with higher pores filling rate can obtain.

The *in vitro* release of ibuprofen under dynamic conditions was performed using a continuous and adjustable flow of phosphate buffer through the sample holder. The intention was to investigate ibuprofen release from the two types of porous calcium phosphate pellets in standardised release conditions. As it is mentioned in a study by Gbureck et al.[43] the drug release rate, especially the initial burst release, depends on the release medium flow rate: for the same drug carrier, drug and release medium, the drug release in static conditions is considerably slower than in dynamic ones. In dynamic conditions, the higher is the flow rate, the faster is the drug release. Therefore, in order to examine the *in vitro* drug release kinetics in conditions approaching the biological situation, the flow rate of the release medium should be decreased at least to 0.46 mL min^{-1}.[44] In the present work, the flow rate was fixed at 2 mL min^{-1}, the minimal flow rate of the flow-through apparatus, leading to a fast ibuprofen release regardless of the carrier composition. Similar dissolution profiles were obtained for both HA and TCP pellets. Only a slight difference in the duration of the second part of the release kinetics was observed, that could stem from the variation in the porosity. Finally, dissolution experiments showed that the total amount of adsorbed ibuprofen was released, confirming that weak Van Der Waals bindings formed between the drug and the substrates. No irreversible drug adsorption occurred, that would have resulted in a total release amount lower than 100%.[45] This indicates that the major factor influencing the ibuprofen release is the type of interactions between the drug and the substrate, which has been shown to be the same for HA and β-TCP. Furthermore, the variation in the pellet porosity did not affect significantly the drug release kinetics.

Besides, the absence of the pellets modification during drug loading and release test indicates that these procedures do not affect the pellets characteristics. Therefore, it can be suggested that after the *in vivo* drug release, these pellets can play their therapeutic role as bone filling materials.

5. Conclusion

The effect of chemical composition of calcium phosphate porous pellets, produced by wet high shear granulation method, on ibuprofen adsorption and release was studied. For this aim HA and β-TCP, two calcium phosphate with different chemical properties, especially different solubility, were compared. Although HA and β-TCP present different chemical properties, the same type of interactions between these pellets and ibuprofen was found. The fast drug uptake, with an adsorption equilibrium time of one hour, and fast and complete ibuprofen release were attributed to ibuprofen physisorption on HA and β-TCP pellets. However, the observed difference in adsorption capacities of HA and β-TCP was found to be controlled by the matrices physical properties, especially their porosity. Thus HA and β-TCP are possible candidates as bone substitutes with anti-inflammatory properties. Based on their similar behaviour towards ibuprofen, the choice of the chemical composition of these pellets would depend on the orthopaedic demands rather than on the drug loading or release limitations. The adsorbed amount of drug could be adapted to the medical need by modulating the physical properties of the pellets *via* the use of another pore former, the adjustment of the pore former amount or the modification of the heat treatment cycle. Indeed, modification of these parameters influences the microstructure and/or pores network.

Acknowledgement

The authors thank the *Région Limousin* for its financial support.

References

1. LeGeros RZ. Properties of osteoconductive biomaterials: calcium phosphates. *Clinical Orthopaedics and Related Research* 2002:81–98.
2. Porter JR, Ruckh TT, Popat KC. Bone tissue engineering: a review in bone biomimetics and drug delivery strategies. *Biotechnology Progress* 2009;**25**:1539–60.
3. Habraken WJEM, Wolke JGC, Jansen JA. Ceramic composites as matrices and scaffolds for drug delivery in tissue engineering. *Advanced Drug Delivery Reviews* 2007;**59**:234–48.
4. Mourino V, Boccaccini AR. Bone tissue engineering therapeutics: controlled drug delivery in three-dimensional scaffolds. *Journal of the Royal Society Interface* 2010;**7**:209–27.
5. Jain AK, Panchagnula R. Skeletal drug delivery systems. *International Journal of Pharmaceutics* 2000;**206**:1–12.
6. Vallet-Regi M, Balas F, Colilla M, Manzano M. Bioceramics and pharmaceuticals: a remarkable synergy. *Solid State Sciences* 2007;**9**:768–76.
7. Vallet-Regi M. Revisiting ceramics for medical applications. *Dalton Transactions* 2006:5211–20.
8. Daculsi G, Malard O, Goyenvalle E. Efficacy and performance of bone substitute for bone reconstruction in place of allograft and autograft. *ITBM-RB* 2005;**26**:218–22.
9. Queiroz AC, Santos JD, Monteiro FJ, Gibson IR, Knowles JC. Adsorption and release studies of sodium ampicillin from hydroxyapatite and glass-reinforced hydroxyapatite composites. *Biomaterials* 2001;**22**:1393–400.
10. Palazzo B, Lafisco M, Laforgia M, Margiotta N, Natile G, Bianchi CL, et al. Biomimetic hydroxyapatite-drug nanocrystals as potential bone substitutes with antitumor drug delivery properties. *Advanced Functional Materials* 2007;**17**:2180–8.
11. Netz DJA, Sepulveda P, Pandolfelli VC, Spadaro ACC, Alencastre JB, Bentley MVLB, et al. Potential use of gelcasting hydroxyapatite porous ceramic as an implantable drug delivery system. *International Journal of Pharmaceutics* 2001;**213**:117–25.
12. Yang P, Quan Z, Li C, Kang X, Lian H, Lin J. Bioactive, luminescent and mesoporous europium-doped hydroxyapatite as a drug carrier. *Biomaterials* 2008;**29**:4341–7.
13. Charnay C, Bégu S, Tourné-Péteilh C, Nicole L, Lerner DA, Devoisselle JM. Inclusion of ibuprofen in mesoporous templated silica: drug loading and release property. *European Journal of Pharmaceutics and Biopharmaceutics* 2004;**57**:533–40.
14. Vallet-Regi M, Ràmila A, Del Real RP, Pérez-Pariente J. A new property of MCM-41: drug delivery system. *Chemistry of Materials* 2001;**13**:308–11.
15. Öner M, Yetiz E, Ay E, Uysal U. Ibuprofen release from porous hydroxyapatite tablets. *Ceramics International* 2011;**37**:2117–25.
16. Palazzo B, Iafisco M, Laforgia M, Margiotta N, Natile G, Bianchi CL, et al. Biomimetic hydroxyapatite-drug nanocrystals as potential bone substitutes with antitumor drug delivery properties. *Advanced Functional Materials* 2007;**17**:2180–8.
17. Chevalier E, Viana M, Cazalbou S, Chulia D. Validation of a manufacturing process of pellets for bone filling and drug delivery. *Journal of Drug Delivery Science and Technology* 2008;**18**:438–44.
18. Chevalier E, Viana M, Cazalbou S, Makein L, Dubois J, Chulia D. Ibuprofen-loaded calcium phosphate granules: combination of innovative characterization methods to relate mechanical strength to drug location. *Acta Biomaterialia* 2010;**6**:266–74.
19. Baradari H, Damia C, Dutreil-Colas M, Champion E, Chulia D, Viana M. β-TCP porous pellets as an orthopaedic drug delivery system: ibuprofen/carrier physicochemical interactions. *Journal of Sience and Technology of Advanced Materials* 2011;**12**:055008, doi:10.1088/1468-6996/12/5/055008.
20. Chevalier E, Viana M, Pouget C, Cazalbou S, Champion E, Chulia D. From porous pellets fabrication to drug loading and release: the case of calcium phosphate matrix loaded with ibuprofen. In: Safford MP, Haines JG, editors. *Bioceramics: properties, preparation and applications in follicular lymphoma and other cancer research*. Nova Sciences Publishers; 2009.
21. Raynaud S, Champion E, Bernache-Assollant D, Thomas P. Calcium phosphate apatites with variable Ca/P atomic ratio I. Synthesis, characterisation and thermal stability of powders. *Biomaterials* 2002;**23**:1065–72.
22. Gracin S, Rasmuson AC. Solubility of phenylacetic acid, p-hydroxyphenylacetic acid, p-aminophenylacetic acid, p-hydroxybenzoic acid, and ibuprofen in pure solvents. *Journal of Chemical and Engineering Data* 2002;**47**:1379–83.
23. Chevalier E, Viana M, Artaud A, Chomette L, Haddouchi S, Devidts G, et al. Comparison of three dissolution apparatuses for testing calcium phosphate pellets used as ibuprofen delivery systems. *AAPS Pharmaceutical Science and Technology* 2009;**10**:597–605.
24. *European pharmacopoeia*. 7th ed. Strasbourg: Council of Europe; 2011.
25. Higuchi T. Mechanism of sustained-action medication: theoretical analysis of rate of release of solid drugs dispersed in solid matrices. *Journal of Pharmaceutical Sciences* 1963;**52**:1145–9.
26. Hixson AW, Crowell JH. Dependence of reaction velocity upon surface and agitation. *Industrial and Engineering Chemistry* 1931;**23**:923–31.
27. Emmett PH, Brunauer S. The use of low temperature van der Waals adsorption isotherms in determining the surface area of iron synthetic ammonia catalysts. *Journal of the American Chemical Society* 1937;**59**:1553–64.
28. Viana M, Jouannin P, Pontier C, Chulia D. About pycnometric density measurements. *Talanta* 2002;**57**:583–93.
29. Moorehead WR, Biggs HG. 2 Amino 2 methyl 1 propanol as the alkalizing agent in an improved continuous flow cresolphthalein complexone procedure for calcium in serum. *Clinical Chemistry* 1974;**20**:1458–60.
30. AFNOR, Implants chirurgicaux — Hydroxyapatite Partie 3: analyse chimique et caractérisation de la cristallinité et de la pureté de phase; 2008.
31. Elliott JC. *Structure and chemistry of the apatites and other calcium orthophosphates*. Amsterdam: Elsevier Science; 1994.
32. Cuscó R, Guitián F, Aza Sd Artús L. Differentiation between hydroxyapatite and β-tricalcium phosphate by means of μ-Raman spectroscopy. *Journal of the European Ceramic Society* 1998;**18**:1301–5.
33. Raynaud S, Champion E, Bernache-Assollant D. Calcium phosphate apatites with variable Ca/P atomic ratio II. Calcination and sintering. *Biomaterials* 2002;**23**:1073–80.
34. Benaziz L, Barroug A, Legrouri A, Rey C, Lebugle A. Adsorption of O-phospho-L-serine and L-serine onto poorly crystalline apatite. *Journal of Colloid and Interface Science* 2001;**238**:48–53.
35. Chevalier E, Viana M, Cazalbou S, Chulia D. Comparison of low-shear and high-shear granulation processes: effect on implantable calcium phosphate granule properties. *Drug Development and Industrial Pharmacy* 2009;**35**:1255–63.
36. Rowe RC. Binder-substrate interactions in granulation: a theoretical approach based on surface free energy and polarity. *International Journal of Pharmaceutics* 1989;**52**:149–54.
37. Iveson SM, Litster JD. Liquid-bound granule impact deformation and coefficient of restitution. *Powder Technology* 1998;**99**:234–42.
38. Litster JD, Hapgood KP, Michaels JN, Sims A, Roberts M, Kameneni SK, et al. Liquid distribution in wet granulation: dimensionless spray flux. *Powder Technology* 2001;**114**:32–9.
39. Naiya TK, Bhattacharya AK, Mandal S, Das SK. The sorption of lead(II) ions on rice husk ash. *Journal of Hazardous Materials* 2009;**163**:1254–64.
40. Stahli C, Bohner M, Bashoor-Zadeh M, Doebelin N, Baroud G. Aqueous impregnation of porous beta-tricalcium phosphate scaffolds. *Acta Biomaterialia* 2010;**6**:2760–72.
41. Hasegawa M, Sudo A, Komlev VS, Barinov SM, Uchida A. High release of antibiotic from a novel hydroxyapatite with bimodal pore size distribution. *Journal of Biomedical Materials Research – Part B: Applied Biomaterials* 2004;**70**:332–9.

42. Seshima H, Yoshinari M, Takemoto S, Hattori M, Kawada E, Inoue T, et al. Control of bisphosphonate release using hydroxyapatite granules. *Journal of Biomedical Materials Research – Part B: Applied Biomaterials* 2006;**78**:215–21.
43. Gbureck U, Vorndran E, Barralet JE. Modeling vancomycin release kinetics from microporous calcium phosphate ceramics comparing static and dynamic immersion conditions. *Acta Biomaterialia* 2008;**4**:1480–6.
44. Nakano T, Thompson JR, Christopherson RJ, Aherne FX. Blood flow distribution in hind limb bones and joint cartilage from young growing pigs. *Canadian Journal of Veterinary Research* 1986;**50**:96–100.
45. Gbureck U, Vorndran E, Müller FA, Barralet JE. Low temperature direct 3D printed bioceramics and biocomposites as drug release matrices. *Journal of Controlled Release* 2007;**122**:173–80.